ADP-ribosylation factor 6 regulates tumor cell invasion through the activation of the MEK/ERK signaling pathway

Sarah E. Tague*†, Vandhana Muralidharan*†, and Crislyn D'Souza-Schorey*‡§

*Department of Biological Sciences and ‡The Walther Cancer Institute, University of Notre Dame, Notre Dame, IN 46556-0369

Communicated by Jack E. Dixon, University of California at San Diego, La Jolla, CA, May 20, 2004 (received for review March 28, 2004)

Tumor cell invasion through the extracellular matrix is accompanied by the formation of invadopodia, which are actin-rich protrusions at the adherent surface of cells at sites of extracellular matrix degradation. Using the invasive human melanoma cell line LOX as a model system, we demonstrate that the ADP-ribosylation factor 6 (ARF6) GTPase is an important regulator of invadopodia formation and cell invasion. We show that ARF6 localizes to invadopodia of LOX cells. Sustained activation of ARF6 significantly enhances the invasive capacity of melanoma as well as breast tumor cell lines, whereas dominant negative ARF6 abolishes basal cell invasive capacity as well as invasion induced by growth factors. Furthermore, using biochemical assays, we show that enhanced invasive capacity is accompanied by the activation of endogenous ARF6. Finally, we provide evidence that ARF6-enhanced melanoma cell invasion depends on the activation of the extracellular signal-regulated kinase (ERK), and that the ARF6 GTPase cycle regulates ERK activation. This study describes a vital role for ARF6 in melanoma cell invasion and documents a link between ARF6-mediated signaling and ERK activation.

An important characteristic of metastasizing cells is their ability to degrade and invade the extracellular matrix. Matrix degradation and cell invasion also occur during normal physiological processes, such as development and differentiation (1). The process of cell invasion is tightly regulated by a number of cell-signaling proteins, such as tyrosine kinases, Ras-related GTPases, and mitogen-activated protein kinase (MAPK) family proteins (2, 3). As an invading cell moves through the extracellular matrix, it extends actin-rich membrane protrusions into the matrix. These protrusions, called invadopodia, contain a number of actin-binding proteins and recruit various proteinases, including matrix metalloproteinases and serine proteases, which degrade matrix proteins at sites of cell invasion (4, 5). Studies on breast cancer and melanoma progression have shown that there appears to be a direct correlation between the ability of cells to form invadopodia and degrade matrix and the cells' invasive potential as measured by *in vitro* and *in vivo* assays for motility and invasion (4, 6, 7).

ADP-ribosylation factor 6 (ARF6) is a member of the Ras superfamily of small GTPases, and like most GTPases, ARF6 alternates between its active GTP-bound and inactive GDP-bound conformations. The ARF6 GTPase cycle has been shown to regulate endosome membrane trafficking, regulated exocytosis, and actin remodeling at the cell surface (8). These processes are important for controlling cell shape changes and can impinge on the acquisition of an invasive phenotype. In fact, previous work in our laboratory has shown that ARF6 promotes cell migration in epithelial cells by facilitating adherens junction disassembly through its effect on endocytosis (of adhesion molecules) and by inducing peripheral actin rearrangements (9). In addition, Santy and Casanova (10) have shown that overexpression of ARNO, a guanine nucleotide exchange factor for ARF6, also induces epithelial cell migration through the downstream activation of phospholipase D and the Rac1 GTPase.

In this study, we have examined the potential involvement of ARF6 during the process of tumor cell invasion. LOX cells, an invasive human amelanotic melanoma cell line, form prominent invadopodia and are capable of degrading gelatin, making it a good model system to study tumor cell invasion (11, 12). We describe an important role for ARF6 in the regulation of invadopodia formation and LOX cell invasion. We find that the activity of endogenous ARF6 increases as cells acquire invasive capacity and that activation of ARF6 is required for both basal level and growth factor-induced cell invasion. Finally, we show that the GTPase cycle of ARF6 regulates extracellular signal-regulated kinase (ERK) activation and that activation of ERK is essential for ARF6-induced melanoma cell invasion. This is the first report that links ARF6-mediated signaling to ERK activation.

Materials and Methods

Cell Lines, Plasmids, and Materials. The human amelanotic melanoma cell line, LOX, was kindly provided by Oystein Fodstad (The Norwegian Radium Hospital, Oslo). The hemagglutinin (HA)-tagged expression plasmids, ARF6(Q67L)–pCDNA3.1(−) and ARF6(T27N)–pCDNA3.1(−), have been previously described (13). Plasmids encoding activated and dominant negative MAPK/ERK kinase 1 (MEK-1) were kindly provided by Andrew Catling and Mike Weber (both from University of Virginia, Charlottesville). The rabbit anti-HA antibody was purchased from Babco (Richmond, CA), and the murine monoclonal anti-HA antibody was purchased from Covance (Princeton). Rhodamine-phalloidin and the murine anti-paxillin antibody were obtained from Molecular Probes. The DS1 polyclonal anti-ARF6 antibody was created from a 12-aa peptide close to the amino-terminal end, as previously described (14). The mouse monoclonal anti-phospho-p44/42 MAPK (Thr-202/Tyr-204) antibody, E10, and the anti- p44/42 MAPK rabbit polyclonal antibody were from Cell Signaling Technology (Beverly, MA), and the anti-transferrin receptor antibody was from Zymed. All secondary antibodies were purchased from Molecular Probes, except the goat anti-rat cy3 antibody, which was purchased from Chemicon. 5-(and-6)-Carboxyfluorescein diacetate, succinimidyl ester (CFDSE) and Texas red-X, succinimidyl ester were purchased from Molecular Probes. The MEK inhibitor, PD98059, was purchased from Calbiochem.

Cell Culture and Transfections. LOX cells were maintained in RPMI medium 1640 supplemented with 10% FBS, 2 mM L-glutamine, penicillin, and streptomycin. Plasmids were transfected into LOX cells via electroporation. LOX cells were trypsinized and washed twice in serum-free medium before electroporation. Cells ($\approx 1.5 \times 10^6$) from exponentially growing cultures were electroporated for 15 s at 230 V and 950 μF with a total of 15 μg of plasmid DNA.

Abbreviations: ARF6, ADP-ribosylation factor 6; CFDSE, carboxyfluorescein diacetate, succinimidyl ester; ERK, extracellular signal-regulated kinase; HA, hemagglutinin; HGF, hepatocyte growth factor; MAPK, mitogen-activated protein kinase; MEK, MAPK/ERK kinase.

†S.E.T. and V.M. contributed equally to this work.

§To whom correspondence should be addressed at: Department of Biological Sciences, University of Notre Dame, Box 369, Galvin Life Sciences Building, Notre Dame, IN 46556-0369. E-mail: D'Souza-Schorey.1@nd.edu.

© 2004 by The National Academy of Sciences of the USA

Electroporated cells were kept in complete RPMI medium 1640 at 37°C in 5% CO_2 for 48 h before further experimentation. Where indicated, LOX cells were also transfected with Metafectene transfection (Biontex Laboratories, Munich), according to the manufacturer's instructions.

Gelatin Degradation Assay. The gelatin degradation assay was modified from a previously published protocol (5). Briefly, coverslips were coated with 1% gelatin and allowed to dry overnight at 4°C. They were then rehydrated for 30 min in 2 ml of sterile H_2O. The gelatin was fixed onto the slide for 30 min with 1% paraformaldehyde. The coated coverslips were washed three times in PBS before being fluorescently labeled with 0.3–0.5 μM CFDSE or 2 μM Texas red-X, succinimidyl ester. The labeled coverslips were washed three times in PBS at 37°C before the seeding of $\approx 2 \times 10^5$ cells in 2 ml of complete RPMI medium 1640 per well. Cells were incubated on gelatin-coated coverslips for 8–24 h as indicated. For experiments with the MEK inhibitor, PD98059, cells were seeded on gelatin along with 18 μM PD98059.

For quantitation of cell invasion, cells were viewed under a fluorescent microscope coupled to a Bio-Rad MRC 1024 scanning confocal three-channel system (see below). For each experimental condition, 150 cells were visualized, and those exhibiting gelatin degradation underneath them were scored. The percentage of cells with gelatin degradation underneath them was calculated as an indicator of cell invasion. The data shown are a mean of three separate experiments.

Measurement of Endogenous ARF6-GTP. LOX cells plated at 80–85% confluency on gelatin-coated 100-mm tissue culture dishes were treated with or without 40 ng/ml HGF (hepatocyte growth factor) for 30–60 min. Analysis of the endogenous ARF6-GTP levels was performed with the MT-2 binding assay as previously described (14).

Immunofluorescent Staining and Microscopy. Immunofluorescent staining and microscopy techniques were conducted as previously described (13) except for staining with the E10 antibody. For immunofluorescent staining with the E10 antibody, cells were fixed and stained as recommended by Cell Signaling Technology. Immunofluorescent imaging was accomplished by using a Bio-Rad MRC 1024 scanning confocal 3 channel system, which uses a krypton–argon laser with excitation filters for 488 nm, 568 nm, and 647 nm and Bio-Rad LASERSHARP 2000 software (version 4.0).

Results

An Experimental System to Visualize Melanoma Cell Invasion. To examine the role of ARF6 in melanoma cell invasion, we used an invasion assay that was modified from a previously published protocol (5). Gelatin was immobilized on glass coverslips and then fluorescently labeled with either CFDSE (green) or Texas red-X, succinimidyl ester (red). LOX cells were seeded on fluorescently labeled gelatin-coated coverslips for 12 h. In the images shown in Fig. 1, LOX cells were labeled for actin, by using rhodamine–phalloidin. Gelatin degradation was visualized as dark spots underneath the cell, and invadopodia were found in areas of degraded gelatin (Fig. 1*A*). In the stacked side projection, invadopodia were observed as membrane protrusions extending into the gelatin (Fig. 1*B*). The number of invadopodia varied from one invading cell to another and appeared to emanate from actin-rich foci at the ventral surface of cells (Fig. 1*C*). These actin foci were also observed on the ventral surface of noninvading cells and may represent dynamic sites of invadopodia biogenesis.

Endogenous ARF6 Localizes to Invadopodia. To initiate our studies with ARF6, we characterized the localization of endogenous ARF6 in LOX cells. LOX cells plated on CFDSE-labeled gelatin-coated coverslips were permeablized and labeled for endogenous ARF6.

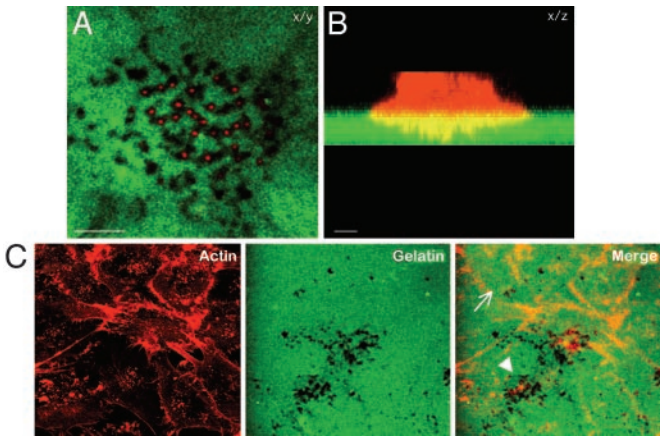

Fig. 1. CFDSE-labeled gelatin is degraded around actin-rich invadopodia formed by LOX cells. LOX cells were seeded on CFDSE-labeled gelatin (green) and allowed to invade for 12 h. The cells were then fixed, permeablized, and stained for actin by using rhodamine phalloidin (red). (*A*) The image on the left is a single confocal plane along the x/y axis at the tips of invadopodia. (*B*) The image on the right is a stacked side projection of the same cell along the x/z axis. (Bar = 10 μm.) (*C*) The image is taken along the ventral cell surface. The number of invadopodia varies from one invading cell to another (compare cells marked by arrow and arrowhead).

ARF6 staining was primarily perinuclear and in tubular compartments that did not overlap with endosomal markers such as the transferrin receptor (Tfn-R) (Fig. 2*A*) or with makers of the Golgi, the endoplamic reticulum, or lysosomes (data not shown). Thus ARF6 does not localize to classical early endosomes in LOX cells as described in Chinese hamster ovary (CHO), human embryonic kidney 293 (HEK293), PC12, and Madin–Darby canine kidney (MDCK) cells (9, 15–17) but to the tubular endosomal compartment that has previously been described in HeLa cells (18). In addition, endogenous ARF6 also localized to membrane protrusions that extended into areas of gelatin degradation (Fig. 2*B*).

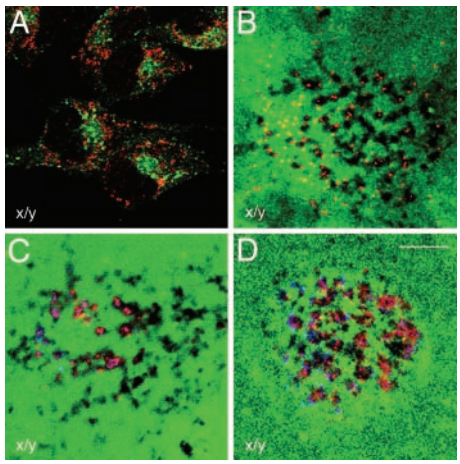

Fig. 2. Endogenous ARF6 localizes to invadopodia along with actin and paxillin. (*A*) LOX cells were processed for immunofluorescence microscopy and labeled for endogenous ARF6 (red) and Tfn-Rs (green). The image is taken across a single confocal plane at the cell body (x/y axis). (*B–D*) LOX cells plated on CFDSE-labeled gelatin (green) were fixed, permeablized, and immunofluorescently labeled for endogenous ARF6 (*B–D*) and actin (*C*), or paxillin (*D*). Images are across a single confocal plane along the x/y axis at the tips of invadopodia. (*B*) Endogenous ARF6 (red) can be seen extending into invadopodia, which are actively degrading gelatin. (*C* and *D*) Actin (red) and paxillin (red) localizes along with endogenous ARF6 (blue) in invadopodia. (Bar = 10 μm.)

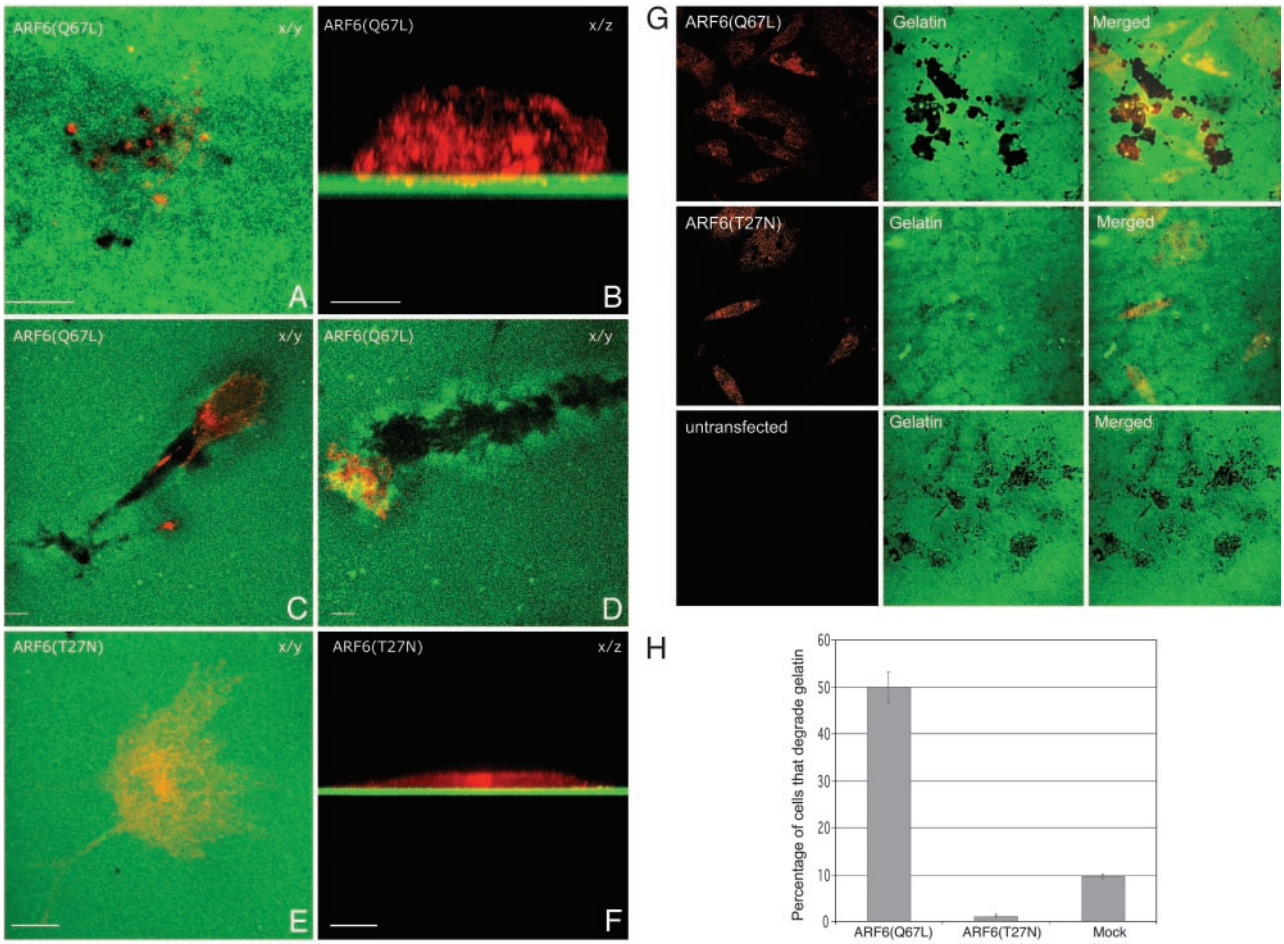

Fig. 3. Constitutively active ARF6 enhances cell invasion, whereas the dominant negative mutant of ARF6 prevents invadopodia formation and gelatin degradation. (*A–F*). LOX cells were transfected with plasmid encoding the HA-tagged ARF6(Q67L) (*A–D*) or the HA-tagged ARF6(T27N) (*E* and *F*). Images are shown along the *x*/*y* (*A* and *C–E*) or *x*/*z* axis (B and *F*). For all images, the HA-tagged ARF6 mutants were immunofluorescently labeled red and the gelatin is green. (Bar = 10 μm.) (*G*) MDA-MB-231 were transfected with plasmid encoding the HA-tagged ARF6(Q67L) or the HA-tagged ARF6(T27N). Images are shown along the *x*/*y* axis. (*H*) Quantitation of cell invasion by ARF6 GTP/GDP mutants. LOX cells were transfected with plasmids as indicated and seeded on gelatin-coated coverslips. After 24 h on gelatin, the percentage of transfected cells with gelatin degradation underneath them was calculated as an indicator of invasion and was compared to the percentage of untransfected cells that exhibited gelatin degradation.

Previous work has shown that invadopodia are actin-rich structures that contain actin-binding proteins and phosphotyrosine (4, 19). Thus, we investigated whether some of these proteins codistributed with ARF6 in invadapodia of LOX cells. In addition to ARF6, actin, paxillin, and phosphotyrosine (data not shown) also were found in invadopodia (Fig. 2 *C* and *D*). The localization of endogenous ARF6 along with these previously identified components of invadopodia suggested that endogenous ARF6 is a bone fide component of invadopodia and may have a functional role in their formation.

The GTPase Cycle of ARF6 Regulates Invasion. To determine the functional significance of the distribution of ARF6 in invadopodia, we examined the effect of disrupting the ARF6 GTPase cycle on cell invasion. For these studies, cells were transfected with HA-tagged expression plasmids encoding the constitutively active, GTPase-deficient mutant of ARF6, ARF6(Q67L), or the dominant negative mutant of ARF6, ARF6(T27N). LOX cells were then seeded on fluorescently labeled, gelatin-coated coverslips and were allowed to invade for 24 h. After fixation, cells were permeablized and immunofluorescently labeled for HA. As previously described for other cell types, ARF6(Q67L), the ARF6-GTP mutant, was diffuse throughout the cell with increased localization at the cell surface, and in invading cells, similar to endogenous ARF6, we found that ARF6(Q67L) was present also in invadopodia (Fig. 3 *A* and *B*). The invading cells appeared more rounded and ≈3–5% of ARF6(Q67L)-transfected cells created "degradation trails." These trails appeared to be formed as cells first invaded down into the gelatin and then continued to degrade through the matrix while moving horizontally (Fig. 3 *C* and *D*; also see Fig. 7, which is published as supporting information on the PNAS web site). This phenotype was not observed in nontransfected cells, and it suggested a more aggressive invasive phenotype for ARF6(Q67L)-transfected cells. In marked contrast, cells expressing the dominant negative ARF6 mutant, ARF6(T27N), remained spread on the gelatin matrix and did not form invadopodia or degrade gelatin (Fig. 3 *E* and *F*). ARF6(T27N) was localized predominantly to the perinuclear cytoplasm. This effect of the ARF6 mutants on cell-invasion capacity was not restricted to melanoma cells but was also observed in the breast tumor cell line MDA-MB-231 (see Fig. 3*G*). In the latter cell line, expression of ARF6(Q67L) resulted in large degradation patches underneath invading cells. Expression of ARF6(T27N) significantly attenuated invasion relative to nontransfected cells, but this inhibition was not complete, and small degradation spots were observed underneath ARF6(T27N)-expressing cells. Because ARF6 appeared to exert more stringent control on

the invasive potential of LOX cells, subsequent studies were performed by using the LOX cell line.

To quantify the invasion efficiencies of LOX cells expressing ARF6 mutants, the percentage of transfected cells with gelatin degradation underneath them were counted and compared to the percentage of nontransfected cells that were degrading gelatin. We found that both ARF6 mutants had a profound effect on LOX cell invasion. As seen in Fig. 3*G*, expression of ARF6(Q67L) promoted gelatin degradation by 5-fold compared to mock-transfected cells, whereas expression of ARF6(T27N) almost completely inhibited gelatin degradation and invasion (Fig. 3*H*). These data indicate a requirement for activated ARF6 in cell invasion.

The structure or number of invadopodia did not appear to be different in cells expressing ARF6-GTP mutant as compared to nontransfected invading cells. It is likely that the rate of turnover of invadopodia is significantly higher in ARF6(Q67L)-expressing cells, leading to a more invasive phenotype. It should be noted that actin foci were also observed at the ventral surface of ARF6(T27N)-expressing cells (see Fig. 8, which is published as supporting information on the PNAS web site). Taken together the above findings suggest that ARF6 activation might serve to control invadopodia formation.

ARF6 Is Required for Invasion Induced by Growth Factors. We investigated whether activated ARF6 might also mediate cell invasiveness induced by a physiologically relevant stimulus. Normal melanocytes require paracrine growth factors from surrounding keratinocytes for proliferation, migration, and survival (20, 21). In contrast, melanoma cells predominantly use autocrine mechanisms and become autonomous (21). Many of the autocrine growth factors up-regulated in melanoma include ligands of receptor tyrosine kinases such as HGF, bFGF (basic fibroblast growth factor), and EGF (epidermal growth factor) as well as G-protein coupled receptor ligands such as α-MSH (α-melanocyte stimulating hormone) (22). We examined the effect of the dominant negative ARF6 mutant on HGF-induced invasion. For these studies, cells transfected with plasmid encoding ARF6(T27N), or those that were mock-transfected, were plated on gelatin and treated with (or without) HGF as described above. As seen in Fig. 4*A*, HGF treatment increased cell invasiveness but not in the presence of ARF6(T27N). These findings indicate that ARF6 is required for events downstream of growth factor-signaling that lead to melanoma cell invasion.

These findings led us to examine whether the activation of endogenous ARF6 was increased upon treatment with HGF. Using a biochemical ARF6-GTP pull-down assay recently developed in our laboratory (14), we examined the levels of activated endogenous ARF6-GTP in HGF-treated and untreated cells. As shown in Fig. 4*B*, endogenous ARF6-GTP levels were significantly increased in "stimulated" cells relative to untreated cells. Thus, there appears to be a direct correlation between ARF6 activation and the acquisition of invasive potential.

ARF6 Regulates ERK Activation in LOX Cells. There is now substantial evidence that the activation of the Ras/Raf/MEK/ERK pathway is vital to melanoma cell invasion (23). The constitutive activation of ERK, a member of the MAPK family, has been identified in almost all invasive melanoma tissues and cell lines tested (23, 24). Furthermore, increased levels of phosphorylated ERK have been associated with increased cell motility, matrix metalloproteinase production, and invasion (3). We therefore analyzed the role of ERK in ARF6-regulated melanoma cell invasion. To this end, we first examined the distribution of phosphorylated ERK in cells expressing the GTP- and GDP-bound mutants of ARF6. Using an antibody that specifically recognizes the dually phosphorylated, activated form of ERK, we found that activated ERK localizes to invadopodia along with ARF6 (Fig. 5 *A* and *B*). Unexpectedly, we also found that the relative levels of phosphorylated ERK were

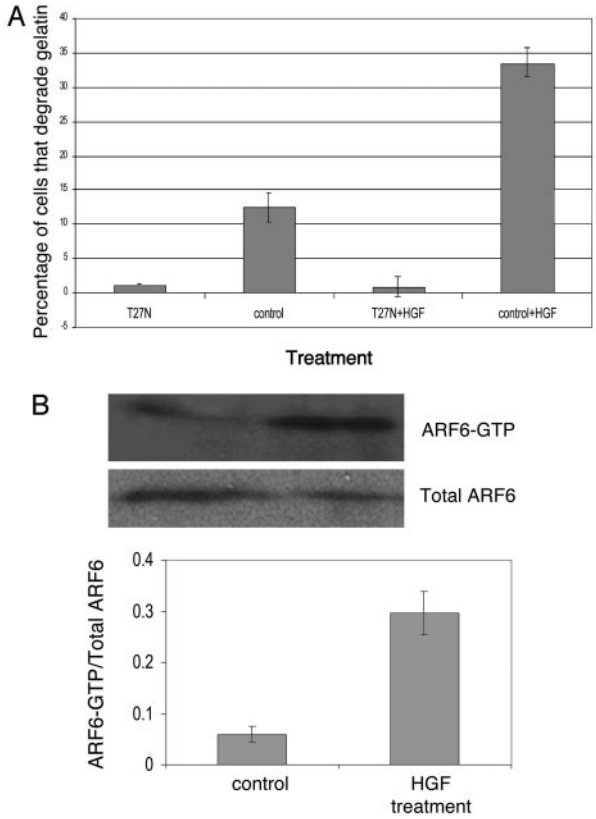

Fig. 4. ARF6 activation is required for and occurs during HGF-induced invasion. (*A*) LOX cells were transfected with plasmids as indicated. Cells plated on CFDSE-labeled gelatin were treated with (or without) 40 ng/ml HGF for 1 h. The percentage of transfected and nontransfected cells with gelatin degradation underneath them was calculated. (*B*) LOX cells were seeded on gelatin-coated tissue culture dishes and treated with or without HGF as described above. Equal amounts of cells lysates from each experimental condition were incubated with GST-MT2 beads to analyze the level of endogenous ARF6-GTP by using procedures previously described (14). Bound ARF6-GTP was visualized by Western blot analysis by using an anti-ARF6 mouse monoclonal antibody. The band densities were measured by using the enhanced UltroScan XL Laser Densitometer (Pharmacia) and the ratio of ARF6-GTP to total ARF6 was calculated. A representative immunoblot of three independent experiments is shown.

significantly higher in ARF6(Q67L)-expressing cells, and significantly lower in ARF6(T27N)-cells compared with nontransfected cells (Fig. 5 *C–H*). We then examined the effect of ARF6 on ERK phosphorylation as well as total ERK levels by using Western blotting procedures. To achieve higher efficiencies of transfection required for the latter set of studies, cells were transfected by using a liposome-based reagent. The latter protocol resulted in 30–40% cell transfection efficiencies. We observed that expression of ARF6(Q67L) augmented ERK activation, whereas the inhibitory effect of ARF6(T27N) on basal levels of ERK activation was not as evident as described above, but likely was masked because of endogenous phospho-ERK in nontransfected cells. However, expression of dominant negative ARF6 significantly inhibited HGF-enhanced ERK activation (Fig. 5*I*). Expression of ARF6 mutants had no effect on total ERK levels. Taken together, these data suggest a previously uncharacterized role for ARF6 in ERK activation.

Inhibition of ERK Signaling Blocks ARF6(Q67L)-Induced Invasion. Next, we investigated whether inhibiting ERK phosphorylation would prevent ARF6(Q67L)-induced invadopodia formation and gelatin degradation. MEK functions directly upstream of ERK, so inhib-

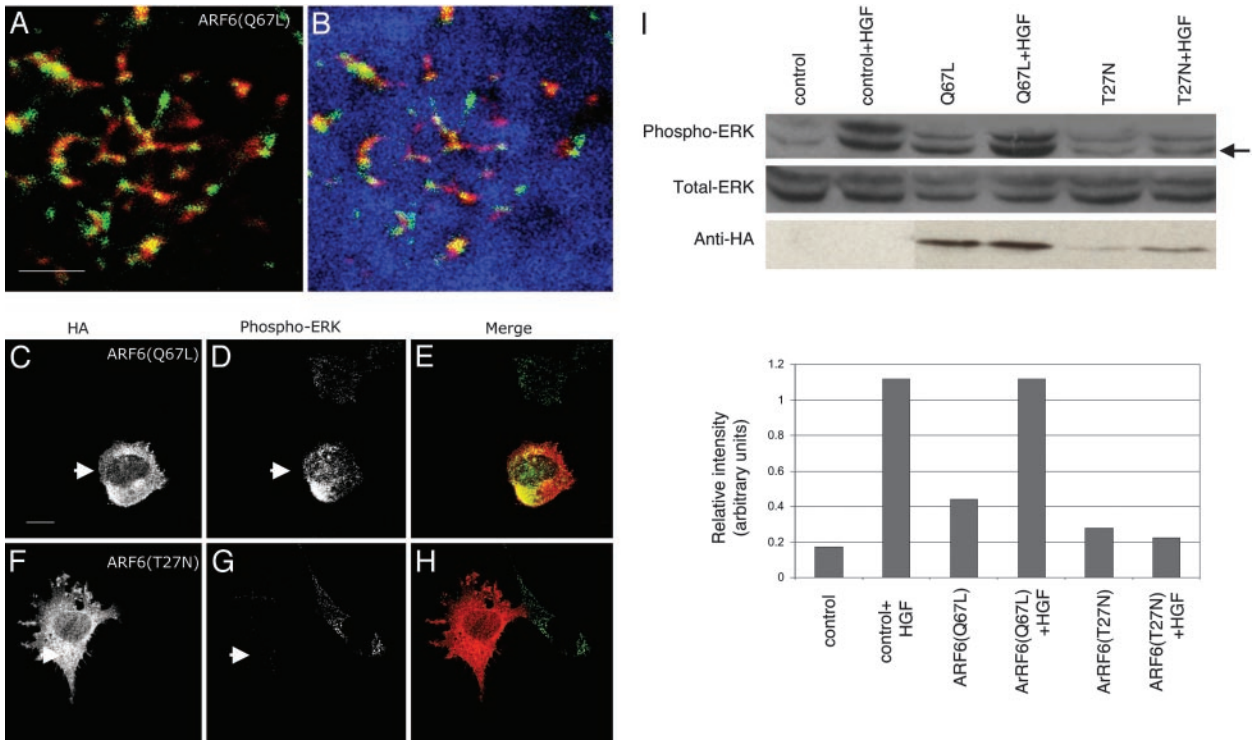

Fig. 5. Activated ARF6 partially colocalizes with activated ERK in invadopodia, and the ARF6 GTPase cycle regulates ERK activation. Cells were transfected as indicated and seeded on CFDSE-labeled gelatin and allowed to invade. Cells were immunofluorescently labeled for HA and/or phosphorylated ERK as indicated. These images were pseudocolored for better visualization of colocalization between ARF6 (red) and phospho-ERK (green). CFDSE-labeled gelatin is pseudocolored blue. (*A* and *B*) Images shown here are single confocal sections at the tips of invadopodia of invading ARF6(Q67L)-expressing cells. *A* is the same as *B* except that *A* does not show gelatin staining. (*C–H*) These images are confocal sections taken along the cell body to better visualize the differences in phospho-ERK levels. Cells were transfected with ARF6(Q67L)-HA (*C–F*) or ARF6(T27N)-HA (*D–G*) and labeled for HA or phospho-ERK as indicated. As seen, ARF6(Q67L)-transfected cells have increased levels of activated ERK (arrows), whereas ARF6(T27N)-transfected cells have decreased levels of activated ERK (arrows) compared with other untransfected cells in the same field. (Bar = 10 μm.) (*I*) LOX cells transfected with plasmids expressing ARF6(Q67L) or ARF6(T27N) or transfected with empty plasmid as control, were plated on gelatin-coated tissue culture dishes, and treated with or without 40 ng/ml HGF for 30 min and lysed. Equal amounts of cell lysates were resolved by SDS/PAGE followed by probing with antisera directed specifically against total ERK, phospho-ERK, or HA. Representative immunoblots of three independent experiments are shown. The relative intensity of lower phospho-ERK band (arrow) was assessed by densitometric scanning.

iting MEK activation will also inhibit ERK activation (25). Thus, LOX cells were transfected with ARF6(Q67L) or mock-transfected and allowed to invade CFDSE-labeled gelatin in the presence of a 18 μM concentration of the MEK inhibitor PD98059 for 24 h. We found that inactivation of MEK abolished ARF6(Q67L)-induced cell invasion and that, noticeably, the cells exhibited a flattened and spread morphological phenotype similar to cells expressing ARF6(T27N), the dominant negative ARF6 mutant (Fig. 6 *A* and *B*). PD98059-treated cells also exhibited actin foci at the ventral surface of cells (data not shown), suggesting that ERK activation occurs downstream of ARF6 to facilitate invadopodia formation from sites at the ventral cell surface. Furthermore, quantitation of invasion efficiencies by scoring the percentage of cells exhibiting gelatin degradation underneath them showed that treatment of PD98059 abolished basal as well ARF6(Q67L)-induced cell invasion (Fig. 6*C*).

To complement the above investigations, we examined the effect of coexpressing a dominant negative MEK-1 mutant, MEK-1S218A, with ARF6(Q67L), and a constitutively activated MEK-1 mutant, S218/222D, with ARF6(T27N). Dually transfected cells that exhibited gelatin degradation underneath them were scored. As seen in Fig. 6*C*, coexpression of dominant negative MEK completely abolished the invasive capacity of ARF6(Q67L)-expressing cells. In contrast, coexpression of dominant negative ARF6(T27N) had no effect on the invasive capacity of cells expressing constitutively activated MEK. Taken together, these studies indicate that ARF6(Q67L) promotes cell invasion at least in part by activating ERK and that ERK activation is essential for melanoma cell invasion.

Discussion

In this study, we have described a critical role for ARF6 in the process of melanoma cell invasion. We have shown that ARF6 regulates invasion in a manner that depends on its GTPase cycle. Sustained activation of ARF6 through the expression of ARF6(Q67L) augmented the invasive potential of the melanoma cell line, LOX, and the expression of a dominant negative ARF6 mutant obliterated cell invasion capacity. In addition to linking ARF6 with the regulation of invasion, this study has also demonstrated a previously unidentified ERK-coupled signaling pathway by which ARF6 exerts its effect on invading cells. Expression of the active form of ARF6 up-regulated the total levels of phosphorylated ERK, whereas expression of the dominant negative mutant of ARF6 down-regulated phospho-ERK levels. Furthermore, we found that ERK activation is essential for ARF6-regulated melanoma invasion.

Although there is accruing evidence that growth factor signaling leading to ERK activation is vital, and even decisive, for the highly metastatic behavior of melanoma, much remains to be understood regarding the molecular events that result in increased ERK activation downstream of growth factor activation during melanoma progression. Activating mutations in N-Ras(Q61L) and

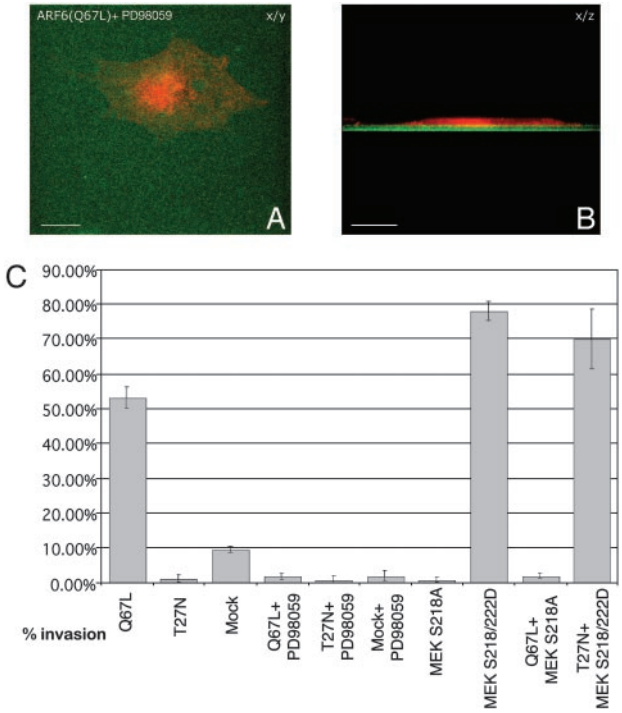

Fig. 6. Inactivation of MEK blocks ARF6-GTP-induced cell invasion. (*A* and *B*) ARF6(Q67L)-transfected cells were seeded on CFDSE-labeled, gelatin-coated coverslips and allowed to invade in the presence of the MEK inhibitor, PD98059. Cells were fixed, permeablized, and immunofluorescently labeled for HA. *A* and *B* are taken along the *x*/*y* and *x*/*z* axis respectively. (Bar = 10 μm.) (*C*) LOX cells were singly or dually transfected with plasmids encoding ARF6 and MEK-1 mutants as indicated. Cells were seeded on gelatin and treated with or without PD98059 as indicated. The percentage of single or dually transfected cells exhibiting gelatin degradation underneath them was scored.

B-Raf(V599E) have been found in the majority of melanoma cell lines and tissues tested (23). (The presence of these mutations in the LOX line is not reported.) However, even when the activating mutation in Ras was not detected in some melanoma cell types, it was still constitutively active. Furthermore, inhibitors of growth factor signaling inhibited ERK activation to varying extents in a variety of melanoma cell lines tested (24). Thus, autocrine signaling and B-Raf activation contribute to increased ERK activation to varying degrees in melanoma.

The regulation of ERK activation through ARF6 is a newly characterized signaling pathway and, in light of the above, could potentially be a critical determinant in melanoma progression. There are a number of pathways by which ARF6 activation may regulate ERK signaling. One interesting mechanism by which ARF6 could increase ERK activation is via its regulation of phospholipid metabolism. Previous studies have shown that PA, a product of PLD metabolism, can stimulate ERK activation (26). Because ARF6 activates PLD (8, 10) this is a feasible means by which ARF6 could regulate ERK activation. Second, ARF6 regulation of PIP2 synthesis (27) could affect ERK activation at sites of invadopodia through the recruitment of scaffolding proteins such as MEKK1, which holds Raf, MEK, and ERK together enabling them to activate one another (28). Interestingly in this regard, we observe a significant build up of PIP2 at invadopodia in ARF6(Q67L)-transfected cells (our unpublished observations). ARF6 may also promote ERK activation through interaction with the paxillin kinase linker (PKL), which has an ARF GTPase-activating protein domain and forms a stable trimolecular complex with PAK and PIX (29). PAK, a direct downstream target of Rac1, is capable of activating Raf and stimulating the Raf-MEK-ERK cascade (30, 31). These are just a few avenues that should be explored in future research.

The studies described here, which characterize an important role for ARF6 in the invasion process, further clarify the pathways that regulate tumor cell invasion. The process of melanoma cell invasion is similar to that observed in bone resorption by osteoclasts, invasion by immune cells, and the initial movement of neural crest cells to the skin before they differentiate into melanocytes, as well as invasion by other types of cancer cells. Thus, ARF6 may prove to be important for these invasive processes as well. Also, by identifying a link between ERK signaling and ARF6, this study paves the way for future investigations on the role of ARF6 in other events regulated by ERK, such as the cell cycle, synaptic and neuronal plasticity, and gene expression.

Note Added in Proof. An article by Hashimoto *et al*. (32) reported a requirement for ARF6 GTPase cycling in breast cancer cell invasion.

We thank Prof. Oystein Fodstad for the LOX cell line; Dr. Victor Hsu for the MDAMB-231 cell line; Dr. Jeff Schorey, Shannon Roach, and Gerry Quinn for sharing reagents and helpful discussions; Dr. Jill Schweitzer for critical reading of the manuscript; Dr. Kun Liang-Guan for helpful discussions; and Kandus Kruger-Passig for excellent technical assistance. This work was supported as a subproject of a Program Project Grant to the Notre Dame–Walther Cancer Center from Department of Defense, U.S. Army Medical Research and Materiel Command.

1. Basbaum, C. B. & Werb, Z. (1996) *Curr. Opin. Cell. Biol.* **8,** 731–738.
2. Hernandez-Alcoceba, R., del Peso, L. & Lacal, J. C. (2000) *Cell Mol. Life Sci.* **57,** 65–76.
3. Klemke, R. L., Cai, S., Giannini, A. L., Gallagher, P. J., de Lanerolle, P. & Cheresh, D. A. (1997) *J. Cell Biol.* **137,** 481–492.
4. Bowden, E. T., Barth, M., Thomas, D., Glazer, R. I. & Mueller, S. C. (1999) *Oncogene* **18,** 4440–4449.
5. Chen, W. T. (1996) *Enzyme Protein* **49,** 59–71.
6. Coopman, P. J., Do, M. T., Thompson, E. W. & Mueller, S. C. (1998) *Clin. Cancer Res.* **4,** 507–515.
7. Chen, W. T., Lee, C. C., Goldstein, L., Bernier, S., Liu, C. H., Lin, C. Y., Yeh, Y., Monsky, W. L., Kelly, T., Dai, M., *et al.* (1994) *Breast Cancer Res. Treat.* **31,** 217–226.
8. Chavrier, P. & Goud, B. (1999) *Curr. Opin. Cell Biol.* **11,** 466–475.
9. Palacios, F., Price, L., Schweitzer, J., Collard, J. G. & D'Souza-Schorey, C. (2001) *EMBO J.* **20,** 4973–4986.
10. Santy, L. C. & Casanova, J. E. (2001) *J. Cell Biol.* **154,** 599–610.
11. Monsky, W. L., Lin, C. Y., Aoyama, A., Kelly, T., Akiyama, S. K., Mueller, S. C. & Chen, W. T. (1994) *Cancer Res.* **54,** 5702–5710.
12. Nakahara, H., Mueller, S. C., Nomizu, M., Yamada, Y., Yeh, Y. & Chen, W. T. (1998) *J. Biol. Chem.* **273,** 9–12.
13. Boshans, R. L., Szanto, S., van Aelst, L. & D'Souza-Schorey, C. (2000) *Mol. Cell. Biol.* **20,** 3685–3694.
14. Schweitzer, J. K. & D'Souza-Schorey, C. (2002) *J. Biol. Chem.* **277,** 27210–27216.
15. D'Souza-Schorey, C., van Donselaar, E., Hsu, V. W., Yang, C., Stahl, P. D. & Peters, P. J. (1998) *J. Cell Biol.* **140,** 603–616.
16. Peters, P. J., Gao, M., Gaschet, J., Ambach, A., van Donselaar, E., Traverse, J. F., Bos, E., Wolffe, E. J. & Hsu, V. W. (2001) *Traffic* **2,** 885–895.
17. Aikawa, Y. & Martin, T. F. (2003) *J. Cell Biol.* **162,** 647–659.
18. Radhakrishna, H. & Donaldson, J. G. (1997) *J. Cell Biol.* **139,** 49–61.
19. Mueller, S. C., Yeh, Y. & Chen, W. T. (1992) *J. Cell Biol.* **119,** 1309–1325.
20. Lazar-Molnar, E., Hegyesi, H., Toth, S. & Falus, A. (2000) *Cytokine* **12,** 547–554.
21. Halaban, R. (1996) *Semin. Oncol.* **23,** 673–681.
22. Bogenrieder, T. & Herlyn, M. (2002) *Crit. Rev. Oncol. Hematol.* **44,** 1–15.
23. Smalley, K. S. (2003) *Int. J. Cancer* **104,** 527–532.
24. Satyamoorthy, K., Li, G., Gerrero, M. R., Brose, M. S., Volpe, P., Weber, B. L., Van Belle, P., Elder, D. E. & Herlyn, M. (2003) *Cancer Res.* **63,** 756–759.
25. Cobb, M. H. (1999) *Prog. Biophys. Mol. Biol.* **71,** 479–500.
26. Hong, J. H., Oh, S. O., Lee, M., Kim, Y. R., Kim, D. U., Hur, G. M., Lee, J. H., Lim, K., Hwang, B. D. & Park, S. K. (2001) *Biochem. Biophys. Res. Commun.* **281,** 1337–1342.
27. Honda, A., Nogami, M., Yokozeki, T., Yamazaki, M., Nakamura, H., Watanabe, H., Kawamoto, K., Nakayama, K., Morris, A. J., Frohman, M. A. & Kanaho, Y. (1999) *Cell* **99,** 521–532.
28. Karandikar, M., Xu, S. & Cobb, M. H. (2000) *J. Biol. Chem.* **275,** 40120–40127.
29. Brown, M. C., West, K. A. & Turner, C. E. (2002) *Mol. Biol. Cell* **13,** 1550–1565.
30. Li, W., Chong, H. & Guan, K. L. (2001) *J. Biol. Chem.* **276,** 34728–34737.
31. Zang, M., Hayne, C. & Luo, Z. (2002) *J. Biol. Chem.* **277,** 4395–4405.
32. Hashimoto, S., Onodera, Y., Hashimoto, A., Tanaka, M., Hamaguchi, M., Yamada, A. & Sabe, H. (2004) *Proc. Natl. Acad. Sci. USA* **101,** 6647–6652.